

# Development of a Mathematical Model and Software for Predicting the Composition and Content of Nonmetallic Oxide Inclusions in Steel in Secondary Steelmaking Processes

A. M. Pogodin<sup>a, \*</sup>, O. A. Komolova<sup>a</sup>, and K. V. Grigorovich<sup>a</sup>

<sup>a</sup> Baikov Institute of Metallurgy and Materials Science, Russian Academy of Sciences, Moscow, Russia

\*e-mail: lpog11@yandex.ru

Received December 3, 2021; revised February 10, 2022; accepted February 17, 2022

**Abstract**—A mathematical model and software based on it have been developed to predict the composition and total content of various types of nonmetallic oxide inclusions (NIs) in steel during secondary steel processing. To create the software, the C++ programming language is used in the Visual Studio environment. As a result, the total oxygen content, the characteristic types of oxide NIs, and their content in metal samples taken at various stages of processing in a ladle–furnace unit (LFU) are determined. To validate the developed mathematical model and software, samples of IF-BH steel, K56, 09G2S, and KEI-55 pipe steels, and austenitic corrosion-resistant 08Kh18N10T steel are studied by fractional gas analysis (FGA) and scanning electron microscopy with electron-probe microanalysis. The agreement between the calculated and experimental FGA data is satisfactory, which indicates an adequacy of the proposed mathematical model of NI formation.

**Keywords:** nonmetallic inclusions, mathematical simulation, pipe steels, IF-BH steel, corrosion-resistant steel, fractional gas analysis, steel quality

**DOI:** 10.1134/S0036029522030090

## INTRODUCTION

Nonmetallic inclusions (NIs) in steels create a significant problem for modern metallurgy because of the negative influence of NIs on the properties of the end product. The degree of NI purity of steel is considered to be one of the main characteristics of its quality, and measures to minimize the NI content in steel form the basis of secondary steelmaking technologies to control the composition and content of NIs at certain stages of production.

The world literature contains extensive information on the comprehensive study of NIs, their composition, the probability of formation, and influence on the properties of alloys. In numerous studies of the influence of NIs on the mechanical and operational properties of steel [1–5], researchers show that NIs, which can be considered as interstitial phases, affect the appearance of thermal and deformation stresses. Micropores form near NIs; as a result of growth and coalescence, they lead to a violation of the integrity of the metal and the formation of microcracks in it [1–3, 5]. Under real operating conditions, products undergo mechanical and thermal stresses, which are taken by the steel matrix–NI system. Since NIs and a steel matrix have dissimilar physical characteristics, such as plasticity (deformability) and linear thermal expansion coefficient (LTEC), their behavior differs [6]. As

a result, due to the presence of NIs in a metal, many of its properties (impact toughness, fatigue failure, machinability) deteriorate [6, 7].

As follows from the concepts of structural fracture mechanics under complex temperature–force operating conditions, fracture can be brittle (without significant plastic deformation) and ductile (plastic deformation at the tip of a propagating crack is comparable with the crack size or the solid body size). They can also affect ductile fracture [8–10], since micropores and then dimples can nucleate around NI particles; their coalescence leads to separation microregions in a metal. The possible formation of discontinuities causes significant deformation of a steel matrix and creates stresses around inclusions, which can fail in time [11].

During deformed in the course of rolling, forging, and stamping, irregularly shaped crystalline NIs play the role of stress concentrators and can cause the formation of cracks, which are the causes of fatigue failure of steel [12].

Plastic inclusions potentially affect plasticity due to their anisotropic behavior and orientation relative to the deformation direction. The presence of plastic inclusions, especially sulfides (such as MnS), can negatively affect the anisotropy of impact strength and fracture toughness, since they deform together with a

steel matrix due to their high plasticity. In addition, plastic inclusions decrease the deformability of steel and its premature failure resistance. Inclusions can significantly decrease the fatigue strength by increasing the tensile stresses [13].

Most oxide NIs of the  $Al_2O_3$  type and calcium aluminates manifest themselves as stress concentrators due to their lower LTEC in comparison with steel [9, 10]. Aluminate inclusions are most dangerous in this regard. These inclusions have sharp edges, do not deform together with a steel matrix, and form stitches [1, 2, 5]. Due to the difference in the LTECs of the base metal and aluminate inclusions, their interfaces become a stress concentration zone, which can lead to the formation of cracks and discontinuities [9, 10].

A high NI content in a steel melt is one of the main causes for clogging steel casting equipment, which leads to a decrease in the steel casting speed and production indicators [14–20].

Inclusions can exert a significant effect on the properties of the rolled surface, causing a degradation in the appearance of the surface, poor polishability, and a decrease in the corrosion resistance (which is especially characteristic of sulfide NIs) and adhesion of a coating [7]. Carbides and oxide inclusions, such as aluminates and silicates, are hard and abrasive, and their presence in steel leads to high wear of cutting tool. On the contrary, large sulfide inclusions act as a lubricant, improving the machinability of automatic steels. The positive effect of NIs on the properties of the end product is also noted when they promote the formation of a fine structure during a phase transformation. For example, titanium-containing oxides are known to serve as potential nucleation centers for the formation of needle ferrite and, hence, to increase the impact strength [21, 22]. In other words, to form a favorable microstructure during solidification and thermomechanical processing, technologists have to provide proper design of the composition of alloys and strict control at the stages of melting, secondary steelmaking, and alloying. The main problem during secondary steelmaking is to perform measures to minimize the NI content in steel.

High-duty steels require strict control of the NI content. To improve the quality of the end product, it is important to have a clear understanding of the mechanism of inclusion formation during steelmaking to control the NI content and size distributions. Such opportunities appear when methods for predicting the formation and removal of NIs in steelmaking, which are based on mathematical simulation, are applied. This is not least due to the fact that the modern world is in transition from the third industrial revolution to the fourth. The fourth industrial revolution, or so-called Industry 4.0, is characterized by the development of digitalization and the introduction of cyber-physical systems. One of the main tools of digitalization is the creation of digital twins. Currently, the

development of various mathematical models of metallurgical processes, both internal (e.g., various chemical reactions in liquid metal bath) and external (supply and addition of appropriate charge materials and reagents) ones, is a challenging problem. The digital twin created by combining these models into a single complex will allow the development of software to optimize technology, to increase the production stability, and to decrease the cost of steel [23].

There are no integral mathematical models simulating the processes of NI nucleation, modification, and growth throughout the technological chain of steelmaking depending on different control actions. The purpose of this study is to develop a mathematical model and software based on it for predicting NI formation in steel during secondary steelmaking. Such software can become one of the components of a digital twin for ladle refining units.

To date, many mathematical models have been developed to describe NI formation at various stages of steel production. Below, we present models [24–40], which describe this process during secondary steelmaking in the most detail.

Mapelli et al. [24] proposed a model to determine the change in the average inclusion size during individual stages of ladle refining and the final sizes of inclusions and their distribution by modeling the mechanisms of their formation, growth, and removal during inert gas blowing of a liquid metal. The model is a single complex consisting of blocks for describing the formation, growth (thermodynamic mode), and removal of inclusions (kinetic mode). The mathematical model [24] was developed to predict the formation and removal of inclusions. For thermodynamic calculations, it uses the following initial data: the chemical composition of steel, the ladle–furnace unit (LFU) volume, the initial temperature, the oxygen content in a metallic melt, the flow rate of argon for blowing a liquid metal, the argon bubble diameter, and the NI radius.

The output data of the model [24], which can be used to improve a technology, are as follows:

- the chemical composition of NIs,
- the number of NIs of a given size.

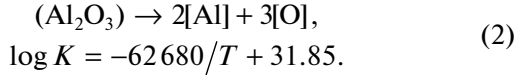
Oxide NIs form if the oxygen activity in a metal [ $a_O$ ] is lower than the oxygen activity in a slag ( $a_{O_s}$ ) [24],

$$\Delta G = RT \ln \frac{(a_O)}{[a_O]} < 0. \quad (1)$$

This model allows calculations for simple oxide NIs of the Fe–Si–Mg–Ca–Al–O system. Based on the Gibbs equation, it is possible to estimate equilibrium constant  $K^{eq}$  for each reaction in the system. Oxide NIs can form inside a liquid metal bath only if  $\Delta G$  in Eq. (1) is negative for each oxide formation reaction.

The Péres [25] describes the formation of  $\text{Al}_2\text{O}_3$ -type oxide NIs and can be used to determine the initial number of formed aluminates. The number of inclusions at the beginning of secondary steelmaking depends on the oxidation level of the metal at tapping before LFU and on the size distribution of inclusions.

This model considers the size distribution of inclusions of the following three groups: small, medium, and large. Inclusions form during the aluminum deoxidation of a metal in accordance with the equation



The number of particles formed depends on the dissolved oxygen content at the end of blowing  $O_{\text{ini}}$  and the dissolved oxygen content after aluminum deoxidation  $O_{\text{eq}}$  [28]. The oxygen activity is calculated as follows:

$$a_{\text{O}} = \left( \frac{10^{-\frac{62680}{T} + 31.85}}{[a_{\text{Al}}]^2} \right)^{1/3}. \quad (3)$$

Taking into account the fact that the activity of any component depends on its content, we use Eq. (3) and find the oxygen content  $O_{\text{eq}}$  in equilibrium with aluminum [25],

$$\%O_{\text{eq}} = \frac{1}{f_{\text{O}}} \left( \frac{10^{-\frac{62680}{T} + 31.85}}{\{[\% \text{Al}] f_{\text{Al}}\}^2} \right)^{1/3}, \quad (4)$$

where  $f_{\text{O}}$  and  $f_{\text{Al}}$  are the activity coefficients of oxygen and aluminum, respectively.

The number of  $\text{Al}_2\text{O}_3$  particles formed according to reaction (2) is calculated as follows [25]:

$$N = \frac{1000(\%O_{\text{ini}} - \%O_{\text{eq}})N_{\text{A}}}{48\rho_{\text{Fe}}}, \quad (5)$$

where 48 is the molecular mass of oxygen (with allowance for three oxygen atoms in each aluminum oxide molecule), g/mol;  $\rho_{\text{Fe}}$  is the steel density, kg/m<sup>3</sup>, 1000 is the conversion factor, and  $N_{\text{A}}$  is Avogadro's number, 1/mol.

The authors of [26] developed a theory to calculate the number of aluminum oxide particles in inclusions of different radii  $R_I$ . To calculate the number  $I$  of particles contained in an inclusion of radius  $R_I$ , the following formula is used [25]:

$$I = (R_I/R_{\text{M}})^3, \quad (6)$$

where  $R_{\text{M}} = 2.719 \times 10^{-10}$  m is the molecular radius of  $\text{Al}_2\text{O}_3$ .

Inclusions of various sizes form from aluminum oxide molecules. The number of particles of each radius  $N_{R_i}$  depends on inclusions of radius  $R_I$ , the fraction  $Z$  of inclusions of each size (value is taken from

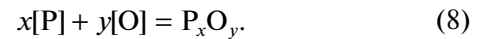
industrial data), and the molecular radius of  $\text{Al}_2\text{O}_3$  ( $R_{\text{M}}$ ). It is calculated as follows [25]:

$$N_{R_i} = Z(O_{\text{ini}} - O_{\text{eq}})N_{\text{A}}/0.048\rho_{\text{Fe}}I. \quad (7)$$

In this model (Eqs. (6), (7)), the possibility of determining the formation of an inclusion of a specific radius is of interest; however, fitting coefficients obtained by a statistical method for a specific unit are used for this purpose.

The authors of [27] considered the formation of NIs during the solidification of a steel matrix paid particular attention to NI formation during secondary steelmaking in the course of liquid metal deoxidation.

The reaction of formation of a simple stoichiometric oxide is usually described by the equation [27]



At a given temperature, the change in the Gibbs energy ( $\Delta G$ ) for reaction (8) is determined as [27]:

$$\Delta G = \Delta G^\circ + RT \ln \left( \frac{a_{\text{P}_x\text{O}_y}}{a_{\text{P}}^x a_{\text{O}}^y} \right). \quad (9)$$

At  $\Delta G = 0$ , reaction (8) reaches an equilibrium state in which the standard change in the Gibbs energy take the following value [27]:

$$\Delta G^\circ = -RT \ln \left( \frac{a_{\text{P}_x\text{O}_y}^{\text{eq}}}{(a_{\text{P}}^{\text{eq}})^x (a_{\text{O}}^{\text{eq}})^y} \right). \quad (10)$$

Then, we have

$$\Delta G = RT \ln \left[ \frac{(a_{\text{P}}^{\text{eq}})^x (a_{\text{O}}^{\text{eq}})^y}{a_{\text{P}}^x a_{\text{O}}^y} \right] \approx -RT \ln \left( \frac{K}{K^{\text{eq}}} \right). \quad (11)$$

Subscript eq in Eqs. (10) and (11) means equilibrium.

If we assume that inclusions are represented by a pure solid oxide phase, the oxide activity is unity ( $a_{\text{P}_x\text{O}_y} = a_{\text{P}_x\text{O}_y}^{\text{eq}} = 1$ ). Therefore, Eq. (9) can be substituted into Eq. (11). In a dilute solution, the change in the Gibbs energy is also estimated by the ratio of the product of concentrations ( $K = C_{\text{P}}^x C_{\text{O}}^y$ ) to the product of solubilities ( $K^{\text{eq}} = (C_{\text{P}}^{\text{eq}})^x (C_{\text{O}}^{\text{eq}})^y$ ), which is called saturation ( $S_{\text{sat}}$ ). This means that inclusions form when the saturation is higher than unity [27].

When describing the formation of inclusions in a melt, the authors of [27] often refer to [28].

If we assume that a spherical core of radius  $r$  forms, the change in the Gibbs energy of the system is determined by the equation [27]

$$\Delta G_{\text{hom}} = \frac{4\pi r^3}{3} \Delta G_{\text{V}} + 4\pi r^2 \sigma_{\text{inL}}, \quad (12)$$

$$r^* = -\frac{2\sigma_{\text{inL}}}{\Delta G_{\text{V}}}, \quad (13)$$

$$\Delta G_{\text{hom}}^* = \frac{16\pi\sigma_{\text{inL}}^3}{3\Delta G_{\text{V}}^2}. \quad (14)$$

In Eq. (12), the first term describes the change in the Gibbs energy of the formation of nucleation centers ( $\Delta G_V$  is the volumetric change in the energy of inclusion formation, which is calculated as the ratio of the molar change in the Gibbs energy to the molar volume of inclusion). The second term in Eq. (12) is the energy barrier induced by the formation of a new interface. Since  $\Delta G_V$  and  $\sigma_{inL}$  (inclusion–liquid steel interface energy) are constant under current conditions, critical radius  $r^*$  for possibly stable inclusion nuclei corresponding to the maximum change in the Gibbs energy during homogeneous nucleation ( $\Delta G_{hom}^*$ ) is obtained by differentiation. These parameters are described in Eqs. (13) and (14) [27]. Moreover, it was found that the core dissolves in a liquid (free energy of the system is minimized) at  $r < r^*$  tends to grow and stabilize at  $r > r^*$ . Thus, the thermodynamics and kinetics of inclusion formation are related to each other.

An expression for describing the nucleation rate was proposed in [29] and improved in [30], and it is the basis for modern data processing,

$$\dot{I} = I_A \exp[-\Delta G_{hom}^*/k_B T]. \quad (15)$$

In Eq. (15),  $I_A$  is the frequency factor, which is determined by the product of the number of centers, the frequency of diffusion of an atom or molecule through the liquid/NI nucleus interface, and the probability of successful adsorption of a particle on a nucleus;  $T$  is the temperature; and  $k_B$  is the Boltzmann constant. To estimate the frequency factor, Turnbull and Fisher [31] proposed the following expression:

$$I_A = \frac{N_A k_B T}{h} \exp\left[-\frac{Q_D}{RT}\right], \quad (16)$$

where  $h$  is Planck's constant and  $Q_D$  is the diffusion activation energy.

With this method, Turpin and Elliot [32] estimated the frequency factor using the following data for several oxides in the iron melt ( $s^{-1} m^{-3}$ ) [33]:  $10^{32}$  for  $Al_2O_3$ ,  $10^{31}$  for  $FeO \cdot Al_2O_3$ ,  $10^{34}$  for  $SiO_2$ , and  $10^{36}$  for  $FeO$ . According to [34], the estimated frequency factor changes in the range  $10^{35} - 10^{45} s^{-1} m^{-3}$ . In their calculations, Turkdogan [35] and Babu et al. [36] took a frequency factor of  $10^{33} s^{-1} m^{-3}$  for oxides. This frequency factor was thought to be considered as a constant in calculations [32, 34–36].

However, according to Eqs. (14) and (15), the nucleation rate is strongly influenced by a change in the Gibbs energy.

Kazakov [37] analyzed NI formation during cooling and solidification of a steel melt and modeled of the formation of titanium nitrides. The model of inclusion formation [37] is of interest primarily because NI formation is considered in a local volume, which is taken to be a dendritic cell, and NI formation was modeled using mass balance equations. This model describes the time dependences of the parameters of formation of titanium oxycarbonitride inclu-

sions over the entire temperature range of steel cooling and solidification. This model makes it possible to trace the dynamics of changing the number and composition of inclusions during melt cooling and solidification and to quantitatively estimate the influence of various factors, including the influence of NIs on dendritic structure formation in steel.

Along with the considered models, we also analyzed other models of NI formation [11, 38–40]. On the whole, the following advantages of all models can be distinguished: they describe and mathematically process the processes of NI formation and removal, the adequacy of the models was confirmed by comparing the results calculated with them with the results of testing industrial samples, and their application makes it possible to determine the number and composition of formed inclusions.

The main limitations of these mathematical models are related to the use of tuning coefficients determined by a statistical method for a specific unit. As a result, they cannot be used for secondary steelmaking units with other characteristics and with other steelmaking technologies. In addition, the models described above do not take into account the oxygen redistribution between components in a liquid metal during NI formation. Moreover, these models, except for the Kazakov model [37], have no material balance equations and use thermodynamic equations to perform calculations over the entire ladle volume, which can lead to less accurate results in predicting NI formation.

## RESULTS AND DISCUSSION

Based on nonequilibrium thermodynamics and material balance equations, we developed a mathematical model to describe the interactions of the components of the NI–metal system. When creating the mathematical model, the following was taken into account:

- (a) in melting and secondary steelmaking, metallurgical systems do not reach equilibrium;
- (b) chemical reactions between the components of the NI–metal system occur simultaneously, and both direct and reverse reactions are possible;
- (c) there is neither chemical composition nor temperature gradient in local volume.

The main feature of this model is that the modeling of the NI formation in a ladle takes into account the redistribution of the components of the NI–metal system. When the NI content is calculated, material balance equations are taken into account and calculations are carried out in the local ladle volume. These factors allow us to obtain more accurate results on calculating the inclusion formation possibility.

When a metal is tapped from an electric arc furnace (EAF) or a converter, the deoxidizers added to a ladle begin to interact with oxygen dissolved in the liquid metal, which leads to the formation of primary oxide NIs. Table 1 gives the reactions of formation of oxide

Table 1. Matrix of oxide NI formation reactions

|                                   | [O]  | [Fe]   | [Mn]   | [Si]  | [Al]  | [Ca]   | [Cr]  |
|-----------------------------------|--|--|--|---|---|--|---|
| [O]                               |  | [Fe] + [O] = (FeO)   | [Mn] + [O] = (MnO)   | [Si] + 2[O] = (SiO <sub>2</sub> )   | 2[Al] + 3[O] = (Al <sub>2</sub> O <sub>3</sub> )                                      | [Ca] + [O] = (CaO)   | [Cr] + [O] = (Cr <sub>2</sub> O <sub>3</sub> )  |
| (FeO)                             | (FeO) = [Fe] + [O]                               |  | [Mn] + (FeO) = (MnO) + [Fe]                                | [Si] + 2(FeO) = (SiO <sub>2</sub> ) + 2[Fe]                               | 2[Al] + 3(FeO) = (Al <sub>2</sub> O <sub>3</sub> ) + 3[Fe]                            | [Ca] + (FeO) = (CaO) + [Fe]                                | 2[Cr] + 3(FeO) = (Cr <sub>2</sub> O <sub>3</sub> ) + 3[Fe]                            |
| (MnO)                             | (MnO) = [Mn] + [O]                               | [Fe] + (MnO) = (FeO) + [Mn]                                |  | [Si] + 2(MnO) = (SiO <sub>2</sub> ) + 2[Mn]                               | 2[Al] + 3(MnO) = (Al <sub>2</sub> O <sub>3</sub> ) + 3[Mn]                            | [Ca] + (MnO) = (CaO) + [Mn]                                | 2[Cr] + 3(MnO) = (Cr <sub>2</sub> O <sub>3</sub> ) + 3[Mn]                            |
| (SiO <sub>2</sub> )               | (SiO <sub>2</sub> ) = [Si] + 2[O]                | 2[Fe] + (SiO <sub>2</sub> ) = 2(FeO) + [Si]                | 2[Mn] + (SiO <sub>2</sub> ) = 2(MnO) + [Si]                |   | 4[Al] + 3(SiO <sub>2</sub> ) = 2(Al <sub>2</sub> O <sub>3</sub> ) + 3[Si]             | 2[Ca] + (SiO <sub>2</sub> ) = 2(CaO) + [Si]                | 4[Cr] + 3(SiO <sub>2</sub> ) = 2(Cr <sub>2</sub> O <sub>3</sub> ) + 3[Si]             |
| (Al <sub>2</sub> O <sub>3</sub> ) | (Al <sub>2</sub> O <sub>3</sub> ) = 2[Al] + 3[O] | 3[Fe] + (Al <sub>2</sub> O <sub>3</sub> ) = 3(FeO) + 2[Al] | 3[Mn] + (Al <sub>2</sub> O <sub>3</sub> ) = 3(MnO) + 2[Al] | 3[Si] + 2(Al <sub>2</sub> O <sub>3</sub> ) = 3(SiO <sub>2</sub> ) + 4[Al] |   | 3[Ca] + (Al <sub>2</sub> O <sub>3</sub> ) = 3(CaO) + 2[Al] | 2[Cr] + (Al <sub>2</sub> O <sub>3</sub> ) = (Cr <sub>2</sub> O <sub>3</sub> ) + 2[Al] |
| (CaO)                             | (CaO) = [Ca] + [O]                               | [Fe] + (CaO) = (FeO) + [Ca]                                | [Mn] + (CaO) = (MnO) + [Ca]                                | [Si] + 2(CaO) = (SiO <sub>2</sub> ) + 2[Ca]                               | 2[Al] + 3(CaO) = (Al <sub>2</sub> O <sub>3</sub> ) + 3[Ca]                            |  | 2[Cr] + 3(CaO) = (Cr <sub>2</sub> O <sub>3</sub> ) + 3[Ca]                            |
| (Cr <sub>2</sub> O <sub>3</sub> ) | (Cr <sub>2</sub> O <sub>3</sub> ) = 2[Cr] + 3[O] | 3[Fe] + (Cr <sub>2</sub> O <sub>3</sub> ) = 3(FeO) + 2[Cr] | 3[Mn] + (Cr <sub>2</sub> O <sub>3</sub> ) = 3(MnO) + 2[Cr] | 3[Si] + 2(Cr <sub>2</sub> O <sub>3</sub> ) = 3(SiO <sub>2</sub> ) + 4[Cr] | 2[Al] + (Cr <sub>2</sub> O <sub>3</sub> ) = (Al <sub>2</sub> O <sub>3</sub> ) + 2[Cr] | 3[Ca] + (Cr <sub>2</sub> O <sub>3</sub> ) = 3(CaO) + 2[Cr] |   |

NIs, which control the oxygen redistribution between the components of the metal melt and oxide phases.

The method of calculating the distribution of oxygen dissolved in metal between the melt components is based on the method described in [14]. For each chemical reaction presented in Table 1, the possibility of formation of an oxide phase is determined and its amount is then calculated.

The NI formation condition is determined by the following ratio [14]:

$$\ln(K_{\text{eq}}/K_{\text{ac}}) > 0, \quad (17)$$

where  $K_{\text{eq}}$  and  $K_{\text{ac}}$  are the equilibrium and actual reaction constants, respectively.

The reaction rates of the interaction of the components in a liquid metal are assumed to be characterized by  $\ln(K_{\text{eq}}/K_{\text{ac}})$ . To calculate the reaction rate of the interactions of the components of the NI–metal system, we developed an algorithm, in which a time unit (1 s) was divided into intervals. The constant of each formation reaction was calculated within an interval (see Table 1). The reaction having the highest value of  $\ln(K_{\text{eq}}/K_{\text{ac}})$  according to Eq. (17) was taken as a basic one. The rate of the basic reaction  $\dot{V}_{\text{bas}}$  per time interval was assumed to be 1 mol/interval. The rates of all other reactions were recalculated relative to the basic one according to the formula [41]

$$\dot{V}_{\text{Me}_x\text{O}_y} = \dot{V}_{\text{bas}} \ln \frac{K_{\text{eq}(\text{Me}_x\text{O}_y)}}{K_{\text{ac}(\text{Me}_x\text{O}_y)}} / \ln \frac{K_{\text{eq,bas}}}{K_{\text{ac,bas}}}. \quad (18)$$

At the end of the cycle, the obtained reaction rates are used to recalculate the material balance, the chemical composition of the metal and NIs, and a transition to the next time interval with new composition characteristics. The cycle is performed until the sum of the values of  $\ln(K_{\text{eq}}/K_{\text{ac}})$  for all chemical reactions reaches the minimum level indicating the impossibility of formation of new oxide inclusions. At the output of the algorithm, information about the types and volume fraction of inclusions, which can form at given secondary steelmaking parameters, can be obtained. Information on the mass, temperature and chemical composition of the metal, as well as its oxidation state, is used as initial data.

Figure 1 shows the block diagram of the algorithm of the mathematical model for simple oxide NI formation. Based on the mathematical model, we created software using the C++ programming language in the Visual Studio environment.

After entering the initial data, the program determines the possibility of nucleation of oxide NIs of each type and allows us to calculate the total content of oxide NIs of each type.

To verify the adequacy of the developed model and to validate it, it is necessary to compare the results of calculations according to the program with the labora-

tory data obtained on estimating the of NI content in steel.

To determine the content of the main types of NIs formed in K56, 09G2S, and KEI-55 pipe steels, corrosion-resistant 08Kh18N10T steel, and IF-BH steel during secondary steelmaking, Grigorovich [42] performed fractional gas analysis (FGA) of metal samples taken at the stages of ladle processing in LFU and from a slab. The study was carried out on a LECO TC600 gas analyzer.

FGA makes it possible to determine the total oxygen and nitrogen content and the amount of oxygen distributed in oxide NIs of different types in a sample and to calculate the volume fraction of oxide NIs.

FGA is a modification of the method of reducing melting in a graphite crucible in a carrier-gas flow at a given linear heating rate of a sample, and it based on the difference between the temperature dependences of the thermodynamic strengths of the oxides in which the major part of oxygen fixed in a metal is located. When the melt temperature increases, the oxides are reduced by carbon from the graphite crucible and oxygen is extracted from the melt in the form of carbon monoxide, and a gas analyzer detects gas release from the sample as a function of a change in the melt temperature. The volume fractions of different types of oxide NIs are calculated using the OxSeP Pro software [43] after introducing data on the chemical composition of the sample.

The use of FGA results in analyzing the influence of technological operations on the number and type of oxide NIs in steel allows us to develop recommendations for the adjustment of technological conditions. The main advantage of FGA is that an analysis provides operational information on the content of total oxygen and nitrogen in a metal and the content of oxygen distributed over different types of NIs [44]. The type of NIs contained in metal samples was evaluated using optical metallography on an OLYMPUS PME 3 microscope integrated into a Thixomet image analysis system. The chemical composition of the inclusions in the samples was analyzed using a Tescan Vega 3SB electron microscope with an Oxford Instruments attachment for electron-probe microanalysis (EPMA).

The LECO TC600 gas analyzer was used to perform FGA of samples of IF-BH steel, K56, 09G2S, and KEI-55 pipe steels; and corrosion-resistant 08Kh18N10T steel. For this purpose, three metal specimens 1.3–1.6 g in weight were taken from each of the IF-BH steel samples (melting technology: converter → LFU → degasser → continuous caster (CC) → slab), which were taken at the beginning of treatment in LFU, before the introduction of deoxidizers, and from a slab, in order to perform parallel operations. An example of the presentation of FGA results is shown in Fig. 2. After processing FGA evolu-

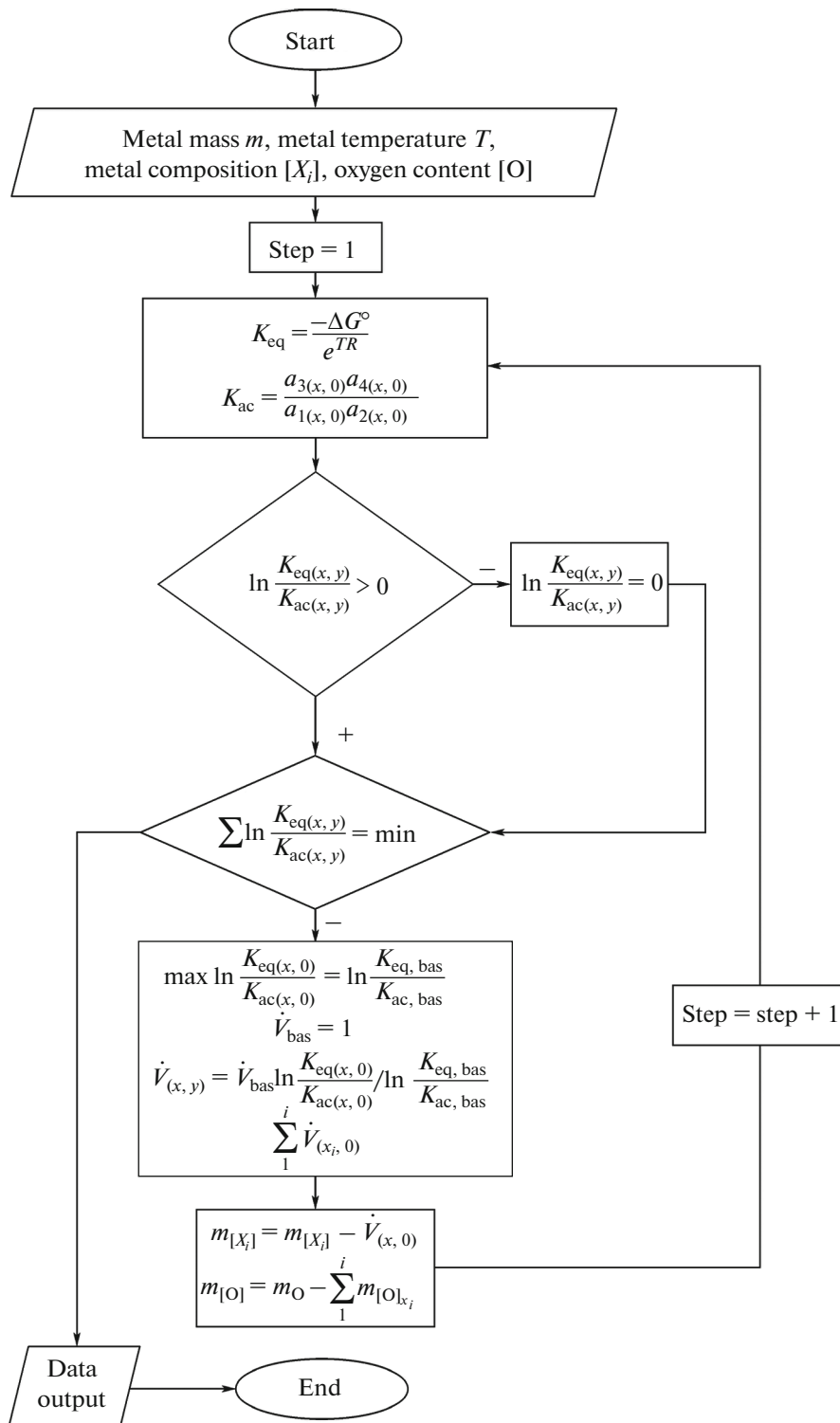


Fig. 1. Flow chart for the algorithm of oxide NI formation.

grams with the OxSeP Pro software, we identified the main types of NIs in the steel samples.

To determine the main types of NIs and to confirm FGA results, the metal samples taken from a slab were

analyzed by EPMA on a scanning electron microscope.

The main sizes of NIs and their compositions were determined by EPMA (Fig. 3). The EPMA data

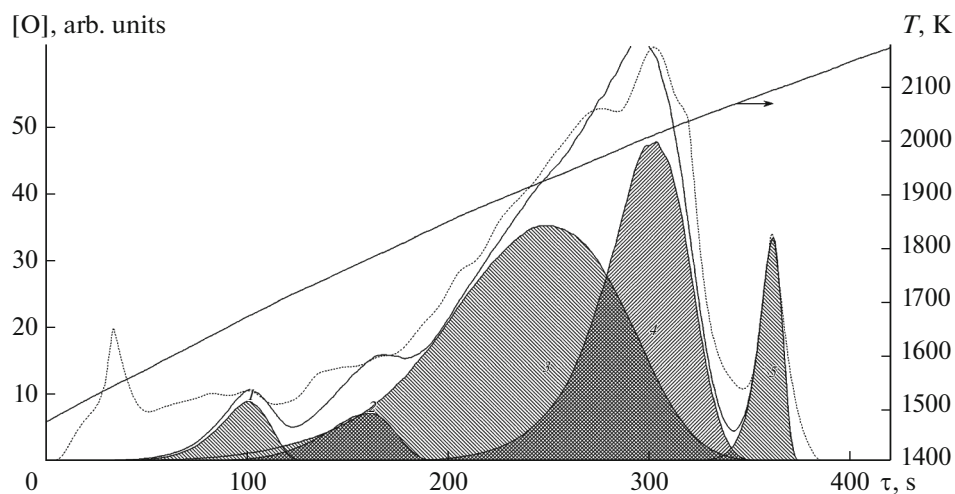


**Fig. 2.** (1–5) Example of determining the oxygen content in oxide NIs in an IF-BH steel sample by FGA and OxSeP Pro calculation.

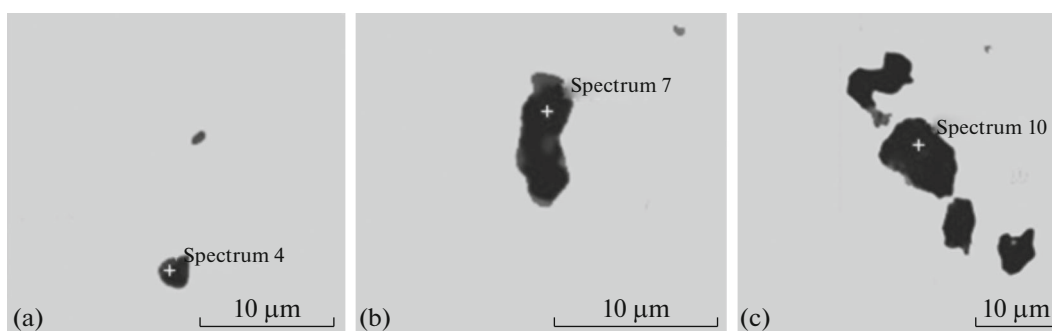


**Fig. 3.** Main groups of NIs in IF-BH steel: (a) silicates (spectrum 4 (at %): 24.1 Si, 19.3 Mn, 17.9 O, 17.0 Fe, 15.1 Al, 5.5 Ca, 0.6 Mg, 0.5 Ti), (b) aluminates (spectrum 7 (at %): 57.4 O, 33.6 Al, 4.4 Fe, 2.6 Ca, 1.1 S, 0.8 Mn, 0.1 Ti), and (c) spinel (spectrum 10 (at %): 63.5 O, 26.8 Al, 3.6 Ca, 2.4 Mg, 1.7 Fe, 1.1 S, 0.5 Mn, 0.3 Si, 0.2 Ti).

demonstrate that the main types of NIs in the samples are aluminates, silicates, and spinel.

Similarly, K56, 09G2S, KEI-55, and 08Kh18N10T steel samples were analyzed; these steels were made according to the technological chain EAF → LFU → degasser → CC → slam. The main types of oxide NIs in the samples were determined by processing the oxygen release curves obtained as a result of FGA of the samples using the OxSeP Pro software package. An example of the presentation of the results of determining the oxygen content in oxide NIs in a K56 pipe steel sample by FGA using the OxSeP Pro software is shown in Fig. 4.

To confirm FGA results, metallographic analysis and EPMA of polished sections of the CC metal samples were carried out. According to the results of the analyses, data were obtained on the main types of NIs, their sizes, and chemical composition in the steels under study. The results of EPMA of the pipe steel samples are shown in Fig. 5. The analysis of NIs con-

firmed the FGA results obtained for the main groups of NIs found in the finished pipe steels.

After receiving EPMA results, we used FGA data to determine the content and type of oxide inclusions in the steel samples under study according to the developed model.

To check the adequacy, FGA results were compared with the calculation results. As the initial data for the calculation according to the program, the chemical compositions according to the results of the first sample from LFU, which were taken from the heat logs of IF-BH steel, K56, 09G2S, and KEI-55 pipe steels, and 08Kh18N10T steel, were used. During the calculation, information was obtained about the total oxygen content in different oxides and about the most likely NIs to be formed. A comparison of the results of FGA of the metal of the first sample taken from each of the three heats on LFU and the results of OxSeP Pro calculation of NI formation in IF-BH steel is presented in Fig. 6.



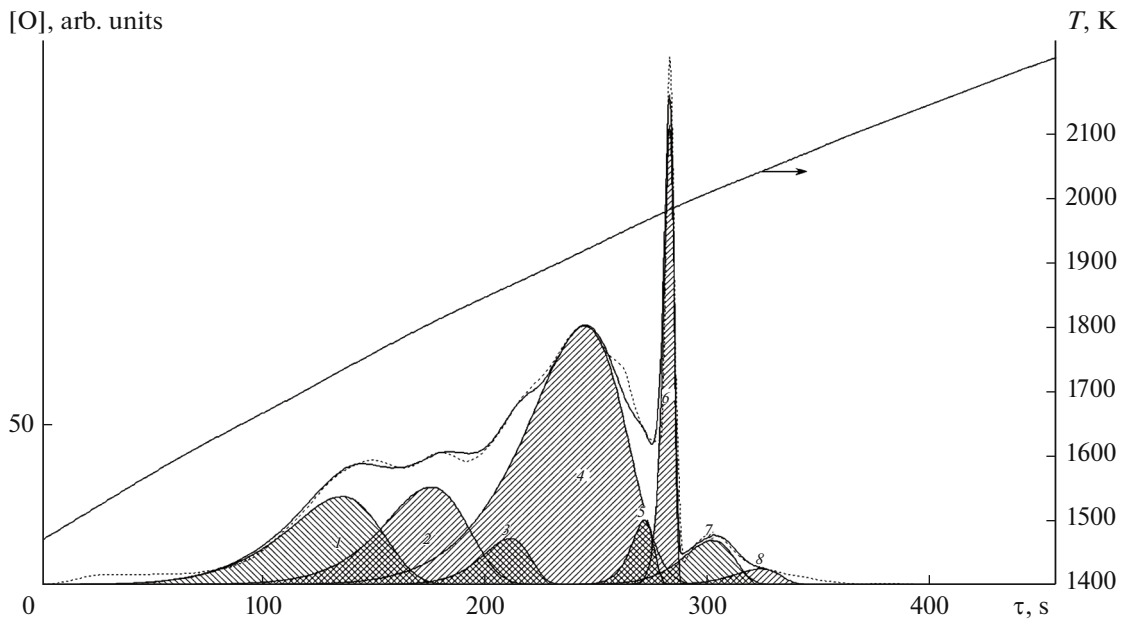


**Fig. 4.** (1–8) Example of determining the oxygen content in oxide NIs in a K56 pipe steel sample by FGA and OxSeP Pro calculation.

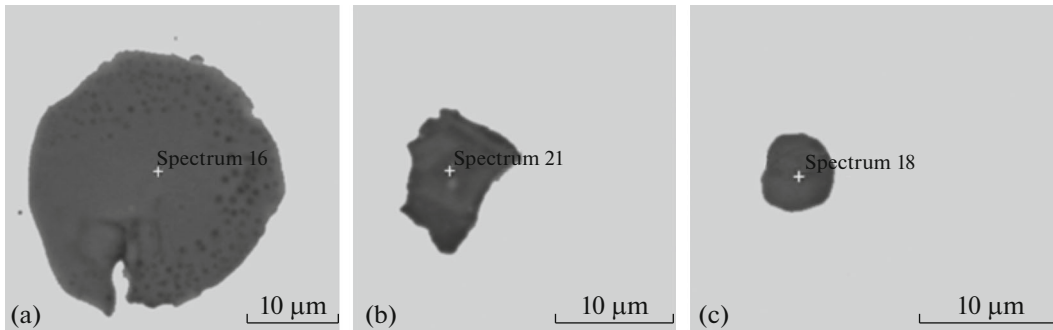
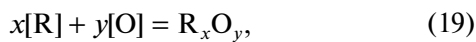


**Fig. 5.** Main groups of NIs in pipe steel: (a) silicates (spectrum 16 (wt %): 43.8 O, 29.8 Mn, 21.3 Si, 3.3 Al, 1.4 Fe, 0.4 Ti), (b) aluminates (spectrum 21 (wt %): 43.0 O, 19.3 Al, 11.7 Mn, 8.2 Si, 7.5 Ti, 3.8 Ca, 3.6 Fe, 1.2 K, 0.9 Cl, 0.8 Na), and (c) spinel (spectrum 18 (wt %): 37.2 Ca, 27.8 O, 17.0 Al, 7.3 S, 4.8 C, 2.6 Fe, 2.1 Mg, 1.2 Si).

A high iron oxide FeO content can be seen in Fig. 6. To verify the obtained data on the FeO content, the following calculation was performed. For the oxide formation reactions



we determined the mass  $m_{[R]}$  (kg) and the amount of substance  $\eta_{[R]}$  (kmol) of component [R],

$$m_{[R]} = [R]m_M/100, \quad (20)$$

$$\eta_{[R]} = m_{[R]}/M_{[R]}, \quad (21)$$

where  $m_M$  is the metal mass (kg), [R] is the content of the oxygen-reacting element [O] (%), and  $M_{[R]}$  is the molar mass of the element [R] (g/mol).

The amount of oxygen [O] (kmol) spent on the complete oxidation of component [R] was determined by the formula

$$\eta_{[O] \rightarrow [R]} = \eta_{[R]}y/x, \quad (22)$$

where  $x$  and  $y$  are the stoichiometric coefficients of Eq. (19).

Using the calculated number of moles  $\eta_{[O] \rightarrow [R]}$ , we determined the mass of oxygen [O] spent on the complete oxidation of component [R],

$$m_{[O] \rightarrow [R]} = \eta_{[O] \rightarrow [R]}M_{[O]}, \quad (23)$$

where  $M_{[O]}$  is the molar mass [O], g/mol.

Based on the initial data on the IF-BH steel composition for the first metal sample from LFU for heat 1 (Table 2), we performed calculations using

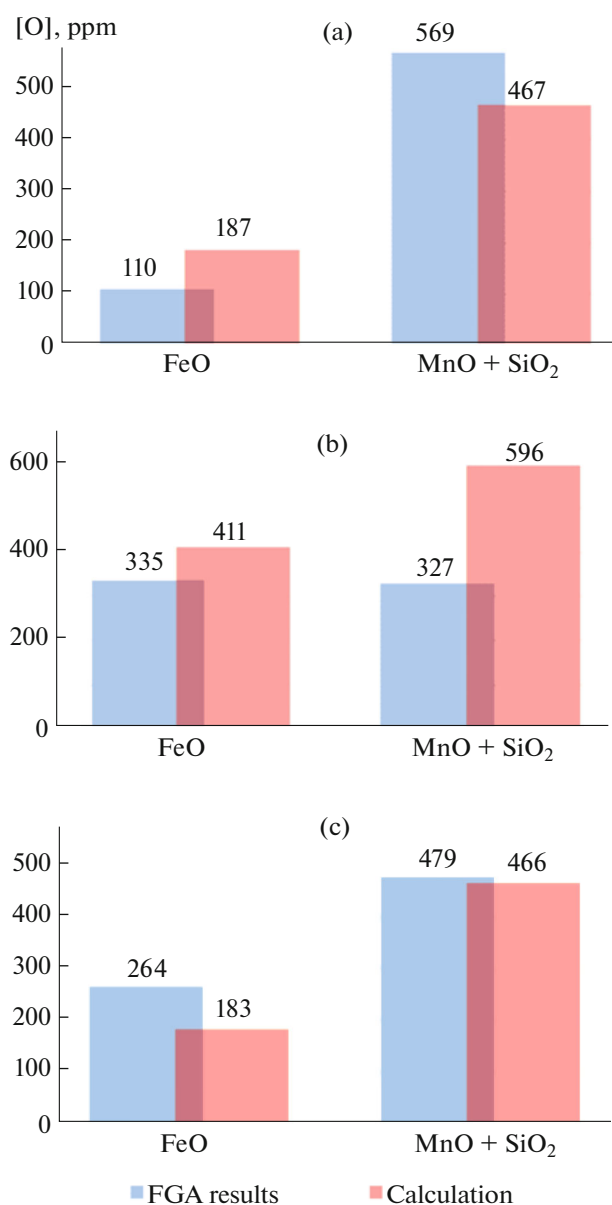


**Fig. 6.** Comparison of the FGA results obtained for samples of three heats ((a–c) heats 1–3) of IF–BH steel for the first metal sample from LFU and the results calculated with the developed program for determining [O] content in oxide NIs of various groups.

Eqs. (19)–(23) and the results of which are given in Table 3.

The calculation results in Table 3 indicate the difference in the oxygen contents  $\Delta[\text{O}] = [\text{O}] - [\text{O}]_{\Sigma}$ , due to which further oxidation of [Fe] occurs after complete oxidation of other components. As a result, FeO-type inclusions are detected in the curves of Fig. 6.

A comparison of the FGA results for the first LFU sample and the calculations using the developed program for determining [O] for the samples of K56, 09G2S, and KEI-55 pipe steels and corrosion-resistant 08Kh18N10T steel is illustrated in Fig. 7.

The results of the model calculations demonstrate good agreement with the FGA results, which allows us to conclude about adequacy of the developed OxSeP Pro software. This software makes it possible to determine the content of simple oxide NIs having formed in a metal during deoxidation in the course of secondary steelmaking, and it can be part of the software package (digital twin), which simulates secondary steelmaking processes [41].

## CONCLUSIONS

(1) The existing materials, works, and publications on the processes of NI nucleation, growth, and removal in steel in the processes of its production were analyzed.

(2) A mathematical model and software based on it were developed to control oxide NI formation in order to predict the total content of NIs having formed during secondary steelmaking as a function of given

**Table 2.** Key component contents (wt %) in IF–BH steel for the first metal sample from LFU for heat 1

| Si     | Al     | Cr     | Mn     | O      |
|--------|--------|--------|--------|--------|
| 0.0040 | 0.0020 | 0.0260 | 0.1700 | 0.0687 |

**Table 3.** Calculated oxygen mass [O] spent on complete oxidation of the components in IF–BH steel for the first metal sample from LFU for heat 1

| Component [R]   | Component content [R], wt % | Component mass $m_{[R]}$ , kg | $m_{[\text{O}] \rightarrow [\text{R}]}$ , kg |
|---|-----------------------------|-------------------------------|--|
| [O]   | 0.0687                      | <b>246.77</b>                 | —  |
| [Si]  | 0.0040                      | 14.37                         | 16.42  |
| [Al]  | 0.0020                      | 7.18                          | 6.38   |
| [Cr]  | 0.0260                      | 93.39                         | 43.10  |
| [Mn]  | 0.1700                      | 610.64                        | 177.64                                       |
| Total oxygen mass $[\text{O}]_{\Sigma}$ spent on complete oxidation of the components, kg |                             |                               | <b>243.54</b>                                |

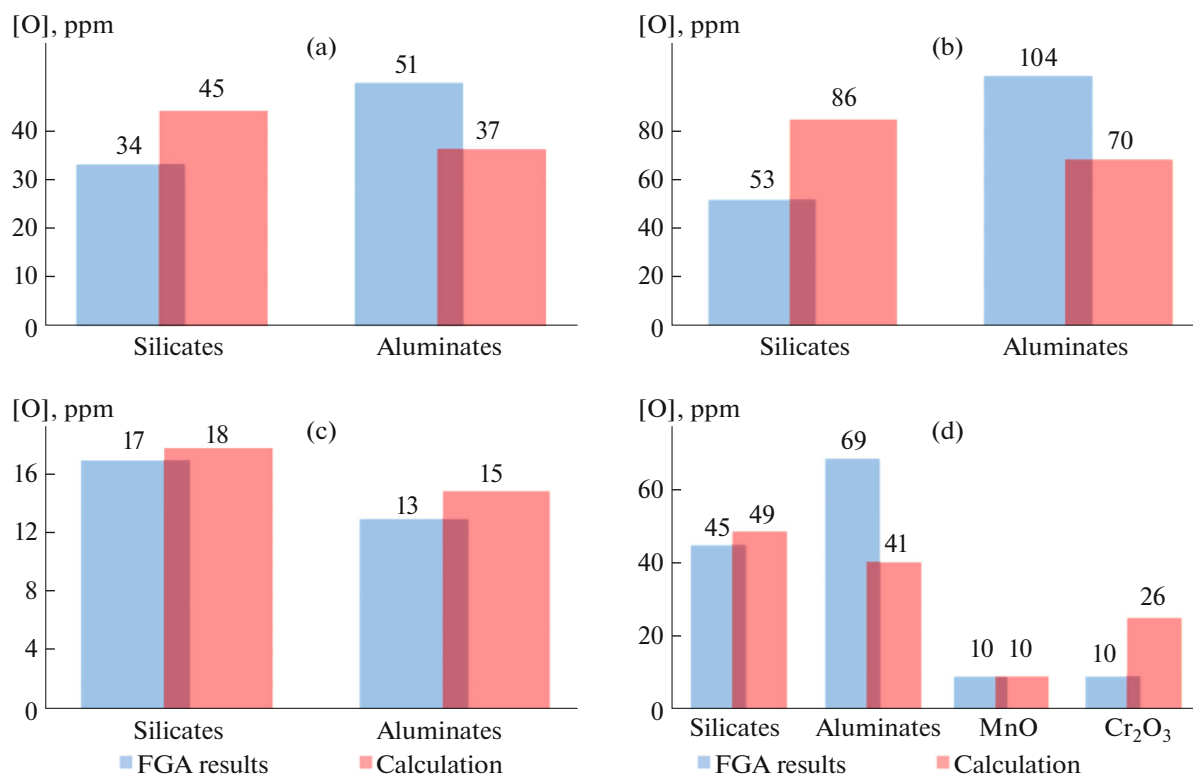


**Fig. 7.** Comparison of the FGA results and the data calculated with the developed program for determining [O] content in oxide NIs of various groups for steels (a) K56, (b) 09G2S, (c) KEI-55, and (d) 08Kh18N10T.

initial conditions (chemical composition, temperature, oxidation, mass of metal and additives).

(3) To validate the developed software and to verify its adequacy, FGA of samples of IF-BH steel, K56, 09G2S, and KEI-55 pipe steels, and corrosion-resistant 08Kh18N10T steel was carried out. FGA results were compared with the results of the software calculation. During an analysis, the main types of NIs found in the metal samples of these steels were identified. The FGA results obtained for the main types of NIs were confirmed by EPMA.

(4) To verify the adequacy of the mathematical model of NI formation and the software developed on its basis, the results of the calculation according to the software package were compared with the FGA results on the number of simple oxide inclusions at the beginning of secondary steelmaking on LFU. The agreement between the calculated and experimental data is satisfactory, which indicates an adequacy of the developed mathematical model.

(5) The developed software makes it possible to determine the possibility of nucleation of simple oxide NIs and their content and will be included in a software package to simulate secondary steelmaking processes.

#### FUNDING

This work was supported by the Russian Foundation for Basic Research, project no. 18-29-24146 mk.

#### CONFLICT OF INTEREST

The authors declare that they have no conflicts of interest.

#### REFERENCES

1. D. Spriestersbach, P. Grad, and E. Kerscher, "Influence of different non-metallic inclusion types on the crack initiation in high-strength steels in the VHCF regime," *Intern. J. Fatigue* **64**, 114–120 (2014).
2. Jian Guan, Liqin Wang, Chuanwei Zhang, and Xinxin Ma, "Effects of non-metallic inclusions on the crack propagation in bearing steel," *Trib. Int.* **106**, 123–131 (2016).
3. A. Gupta, S. Goyal, K. A. Padmanabhan, and A. K. Singh, "Inclusions in steel: micro-macro modeling approach to analyze the effects of inclusions on the properties of steel," *Int. J. Adv. Manufactur. Technol.* **77** (1–4), 565–572 (2014).
4. M. A. Shtremel, "Problems of the metallurgical quality of steel (nonmetallic inclusions)," *Metal Sci. Heat Treat.* **22** (8), 539–544 (1980).

5. C. Mapelli, "Non-metallic inclusions and clean steel," *Met. Italiana*. **6**, 43–52 (2008).
6. A. Ghosh, in *Secondary Steelmaking: Principles and Applications* (CRC Press, Boca Raton, 2000), pp. 255–274.
7. A. Nicholson and T. Gladman, "Non-metallic inclusions and developments in secondary steelmaking," *Ironmak. & Steelmak.* **13** (2), 53–69 (1986).
8. H. V. Atkinson and G. Shi, "Characterization of inclusions in clean steels: a review including the statistics of extremes methods," *Prog. Mater. Sci.* **48** (5), 457–520 (2003).
9. P. Ghosh, C. Ghosh, and R. K. Ray, "Precipitation in interstitial free high strength steels," *ISIJ Int.* **49** (7), 1080–1086 (2009).
10. Lifeng Zhang, Qiang Ren, Haojian Duan, Ying Ren, Wei Chen, Gong Cheng, Wen Yang, and S. Sridhar, "Modeling of non-metallic inclusions in steel," *Miner. Proc. Extract. Met.* **129** (2), 184–206 (2020).
11. T. A. Engh, in *Principles of Metal Refining* (Oxford University Press, Oxford, 1992), pp. 19–38.
12. D. A. Dyudkin and V. V. Kisilenko, *Steelmaking. Vol. 1. Melting, Secondary Steelmaking, and Continuous Casting* (Teplotekhnika, Moscow, 2008).
13. D. Brooksbank and K. W. Andrews, "Stress field around inclusions and their relations to mechanical properties," *J. Iron and Steel Inst.* **210**, 246–255 (1972).
14. A. O. Morozov, A. M. Pogodin, O. A. Komolova, K. B. Bikin, and K. V. Grigorovich, "Control of oxide nonmetallic inclusions during the production of IF steel," *Izv. Vyssh. Uchebn. Zaved., Chern. Metall.* **63** (10), 782–790 (2020).  
<https://doi.org/10.17073/0368-0797-2020-10-782-790>
15. Ying Ren, Lifeng Zhang, and Shusen Li, "Transient evolution of inclusions during calcium modification in linepipe steels," *ISIJ Int.* **54** (12), 2772–2779 (2014).
16. P. Ghosh, C. Ghosh, and R. K. Ray, "Precipitation in interstitial free high strength steels," *ISIJ Int.* **49** (7), 1080–1086 (2009).
17. W. V. Bielefeldt and A. C. F. Vilela, "Study of inclusions in high sulfur, Al-killed Ca-treated steel via experiments and thermodynamic calculations," *Steel Res. Int.* **85** (9999), 1–11 (2014).
18. F. Tehovnik, J. Burja, B. Arh, and M. Knap, "Submerged entry nozzle clogging during continuous casting of Al-killed steel," *Metalurgija*, No. 54 (2), 371–374 (2015).
19. J. Li, G. Cheng, Q. Ruan, J. Pan, and X. Chen, "Evolution behaviour of nonmetallic inclusions in Ti-bearing 11Cr stainless steel with calcium treatment," *Ironmak. & Steelmak.* **47** (1), 1–9 (2020).
20. J. Ikäheimonen, K. Leiviskä, J. Ruuska, and J. Matkalla, "Nozzle clogging prediction in continuous casting of steel," in *Proceedings of 15th Triennial World Congress* (Barcelona, 2002), pp. 143–147.
21. Y. Sahai and T. Emi, in *Tundish Technology for Clean Steel Production* (World Scientific, Singapore, 2008), pp. 43–46.
22. R. Dekkers, B. Blanpain, P. Wollants, F. Haers, B. Gommers, and C. Verduyssen, "A morphological comparison between inclusions in aluminium killed steels and deposits in submerged entry nozzle," *Steel Res. Int.* **74** (6), 351–355 (2003).
23. K. V. Griogorovich and O. A. Komolova, "On the role of physicochemical studies and mathematical simulation in modern metallurgy," in *Proceedings of International Conference on Physicochemical Fundamentals of Metallurgical Processes Dedicated to the 115th Anniversary of Academician A.M. Samarin* (Moscow, 2019), p. 17.
24. C. Mapelli, S. Barella, A. Gruttadauria, and D. Mombelli, "Prevision of inclusion content in structural steel," in *Proceedings of 5th International Congress on the Science and Technology of Steelmaking 2012* (Dresden, 2012), pp. 1–9.
25. J. Pérez, *Inclusion Control Model in Ladle Metallurgy Furnace. Master's Thesis* (McMaster University, Ontario, 2012).
26. L. Zhang, W. Pluschkell, and B. Thomas, "Nucleation and growth of alumina inclusion during deoxidation," in *Proceedings of 85th Steelmaking Conference* (Nashville, 2002), Vol. 85, pp. 463–476.
27. D. You, S. K. Michelic, P. Presoly, J. Liu, and C. Bernhard, "Modeling inclusion formation during solidification of steel," *Review. Metals* **7** (11), 1–31 (2017).  
<https://doi.org/10.3390/met7110460>
28. J. W. Christian, *The Theory of Transformations in Metals and Alloys* (Pergamon, Oxford, 2002).
29. M. Volmer and A. Weber, "Keimbildung in übersättigten gebilden," *Z. Phys. Chem.* **119**, 277–301 (1926).
30. R. Becker and W. Döring, "Kinetische behandlung der keimbildung in übersättigten dämpfen," *Ann. Phys.* **416**, 719–752 (1935).
31. D. Turnbull and J. C. Fisher, "Rate of nucleation in condensed systems," *J. Chem. Phys.* **17**, 71–73 (1949).
32. M. L. Turpin and J. F. Elliott, "Nucleation of oxide inclusions in iron melts," *J. Iron Steel Inst.* **204**, 217–225 (1966).
33. J. F. Elliott, M. Gleiser, and V. Ramakrishna, *Thermochemistry for Steelmaking: Thermodynamic and Transport Properties* (Addison-Wesley, 1963), Vol. 2.
34. P. Rocabois, J. Lehmann, H. Gaye, and M. Wintz, "Kinetics of precipitation of non-metallic inclusions during solidification of steel," *J. Cryst. Growth* **198**, 838–843 (1999).
35. E. T. Turkdogan, "Nucleation, growth, and flotation of oxide inclusions in liquid steel," *Iron Steel Inst.* **204**, 914–919 (1966).
36. S. S. Babu, S. A. David, J. M. Vitek, K. Mundra, and T. Debroy, "Development of macro- and microstructures of carbon–manganese low alloy steel welds," *Mater. Sci. Technol.* **11**, 186–199 (1995).
37. A. A. Kazakov, "Nonmetallic inclusions in steel. Theory and its applications," *Perspekt. Mater.* **VI**, 203–275 (2017).
38. Joo Hyun Park and Dong-Jin Kim, "Formation of inclusions in high Mn–Al steels (HiMAS) and the reac-

- tion between calcium silicate slag and HiMAS melts,” in *Proceedings of 5th International Congress on Science and Technology of Steelmaking ICS 2012* (ICS, Dresden, 2012), p. 165.
39. V. Seshadri, António da Silva C., and Alves da Silva I., “A physical modeling study of inclusion removal in tundish using inert gas curtain,” *Technol. Metal. Mater. Miner.* **9** (1), 22–29 (2012).
40. H. Ling, L. Zhang, and H. Li, “Mathematical modeling on the growth and removal of non-metallic inclusions in the molten steel in a two-strand continuous casting tundish,” *Met. Mater. Trans. B* **47** (5), 2991–3012 (2016).
41. K. Grigorovich and O. Komolova, “Dynamic simulation of ladle treatment process of steel—new software and method for technology optimization,” in *Proceedings of 6th International Congress on Science and Technology of Steelmaking ICS 2015* (ICS, 2015), pp. 354–357.
42. K. V. Grigorovich, “Fractional analysis of oxygen in metals—method features and possibilities,” *Analitika Kontrol* **6** (2), 151–159 (2002).
43. K. V. Grigorovich, P. V. Krasovskii, S. A. Isakov, A. A. Gorokhov, and A. S. Krylov, “Processing and interpretation of fractional gas analysis results,” *Zavod. Lab.* **68** (9), 3–9 (2002).
44. K. Grigorovich, O. Komolova, and D. Terebikina, “Analysis and optimization of ladle treatment technology of steels processing,” *J. Chem. Technol. Metall.* **50** (6), 574–580 (2015).

*Translated by K. Shakhlevich*